Ultrahigh-pressure polyamorphism in GeO_2 glass with coordination number >6

Yoshio Kono[a,1], Curtis Kenney-Benson[a], Daijo Ikuta[a], Yuki Shibazaki[b], Yanbin Wang[c], and Guoyin Shen[a]

[a]High Pressure Collaborative Access Team, Geophysical Laboratory, Carnegie Institution of Washington, Argonne, IL 60439; [b]Frontier Research Institute for Interdisciplinary Sciences, Tohoku University, Aoba-ku, Sendai 980-8578, Japan; and [c]Center for Advanced Radiation Sources, The University of Chicago, Chicago, IL 60637

Edited by Alexandra Navrotsky, University of California, Davis, CA, and approved February 17, 2016 (received for review December 9, 2015)

Knowledge of pressure-induced structural changes in glasses is important in various scientific fields as well as in engineering and industry. However, polyamorphism in glasses under high pressure remains poorly understood because of experimental challenges. Here we report new experimental findings of ultrahigh-pressure polyamorphism in GeO_2 glass, investigated using a newly developed double-stage large-volume cell. The Ge–O coordination number (CN) is found to remain constant at ∼6 between 22.6 and 37.9 GPa. At higher pressures, CN begins to increase rapidly and reaches 7.4 at 91.7 GPa. This transformation begins when the oxygen-packing fraction in GeO_2 glass is close to the maximal dense-packing state (the Kepler conjecture = ∼0.74), which provides new insights into structural changes in network-forming glasses and liquids with CN higher than 6 at ultrahigh-pressure conditions.

high pressure | polyamorphism | glass | oxygen packing

Understanding the structural response of network-forming glasses to pressure is of great interest not only in condensed matter physics, geoscience, and materials science, but also in engineering and industry. As prototype network-forming glasses, silica (SiO_2) and germania (GeO_2) have been the most extensively studied (1–5). These two glasses have similar structural change pathways at high pressures. At ambient pressure, both glasses are composed of corner-linked AO_4 tetrahedra, with atom A (Si or Ge) in fourfold coordination (6). Under compression, the coordination gradually changes from 4 to 6 over a wide pressure range [∼15–40 GPa for SiO_2 glass (2, 4) and ∼5–15 GPa for GeO_2 glass (1, 3, 5)].

A recent study (7) found that evolution of network-forming structural motifs in glasses and liquids at high pressures can be rationalized in terms of oxygen-packing fraction (OPF). Fourfold-coordinated structural motifs in SiO_2 and GeO_2 glasses are stable over a wide range of OPF between 0.40 and ∼0.59. The fourfold-coordinated structural motifs become unstable when the OPF approaches the limit of random loose packing of hard spheres (0.55–0.60) (8, 9). When OPF >∼0.60, coordination number (CN) gradually increases with OPF to the limit of random close packing (0.64) (8, 9), where CN increases sharply to 6 with almost-constant OPF ∼0.64. Higher-pressure data for SiO_2 glass suggest the existence of another stability plateau for sixfold-coordinated structural motifs, with OPF of up to ∼0.72 (7).

The highest coordination that has been experimentally determined so far in SiO_2 and GeO_2 glasses is 6. X-ray diffraction measurement for SiO_2 glass confirmed that sixfold-coordination structural motifs are stable up to 100 GPa (4). For GeO_2 glass, X-ray and neutron diffraction data are limited to 18 GPa (1, 3, 5). X-ray absorption spectroscopic measurements were conducted to 64 GPa (10, 11). Ref. 11 showed no major change in X-ray absorption fine structure up to 64 GPa, although a slight discontinuous change in density is observed around 40–45 GPa.

Some simulation studies predicted the existence of structural motifs with CN >6 above ∼100 GPa for SiO_2 liquid (12) and glass (13) and above ∼60 GPa for GeO_2 glass (13), with no experimental confirmation so far. A study (14) of SiO_2 glass using Brillouin scattering in a diamond anvil cell (DAC) showed a kink in the pressure dependence of shear-wave velocity at ∼140 GPa and was interpreted as evidence of ultrahigh-pressure polyamorphism in SiO_2. However, no structural information is available under such high pressures. In this study, we developed a new double-stage cell, which enables us to study structure of GeO_2 glass at in situ high-pressure conditions up to 91.7 GPa.

Large-volume samples are vital for accurate measurements on the structure of glasses at high pressures using X-ray diffraction because of the weak X-ray scattering from amorphous materials. In such measurements, a large diffraction angle is essential for accurately determining the structure factor with sufficiently large coverage of momentum transfer Q ($Q = 4\pi E\sin\theta/12.398$, where E is X-ray energy in keV and θ is the diffraction angle), and for high resolution in the reduced pair distribution function in real space. Recently, generation of pressure up to 94 GPa has been achieved in a DAC with 1-mm culet size anvils (15). However, this large-volume DAC is designed for neutron diffraction measurement; it is difficult to apply this apparatus for X-ray diffraction measurement because of limited solid-angle access. Similarly, there have been attempts to generate high pressures by inserting diamond anvils inside multianvil large-volume presses (16, 17). However, multianvil presses generally have even more limited solid-angle access for X-ray diffraction signals.

We have developed a new double-stage Paris–Edinburgh (PE)-type large-volume press to generate high pressures with large sample volume (Fig. 1*A*). A pair of second-stage diamond anvils is introduced into the first-stage PE anvils. This combination of opposed anvils (both first- and second stage) provides a large opening in the horizontal plane for X-ray diffraction measurement. To reduce absorption of the gasket surrounding the sample, we used a cubic boron nitride + epoxy (10:1 in weight ratio) inner

Significance

A new double-stage large-volume cell was developed to compress large GeO_2 glass samples to near 100 GPa and to conduct multiangle energy-dispersive X-ray diffraction measurement for in situ structure measurements. We find new experimental evidence of ultrahigh-pressure polyamorphism in GeO_2 glass with coordination number (CN) significantly >6. The structural change to CN higher than 6 is closely associated with the change in oxygen-packing fraction. Our results provide direct structural evidence for ultradense network-forming glasses and liquids. The observed ultrahigh-pressure polyamorphism may also exist in other network-forming glasses and liquids as well, such as SiO_2 and other silicate and germanate systems.

Author contributions: Y.K. and G.S. designed research; Y.K., C.K.-B., and Y.S. performed research; Y.K., D.I., Y.W., and G.S. analyzed data; and Y.K. wrote the paper.

The authors declare no conflict of interest.

This article is a PNAS Direct Submission.

[1]To whom correspondence should be addressed. Email: ykono@ciw.edu.

This article contains supporting information online at www.pnas.org/lookup/suppl/doi:10.1073/pnas.1524304113/-/DCSupplemental.

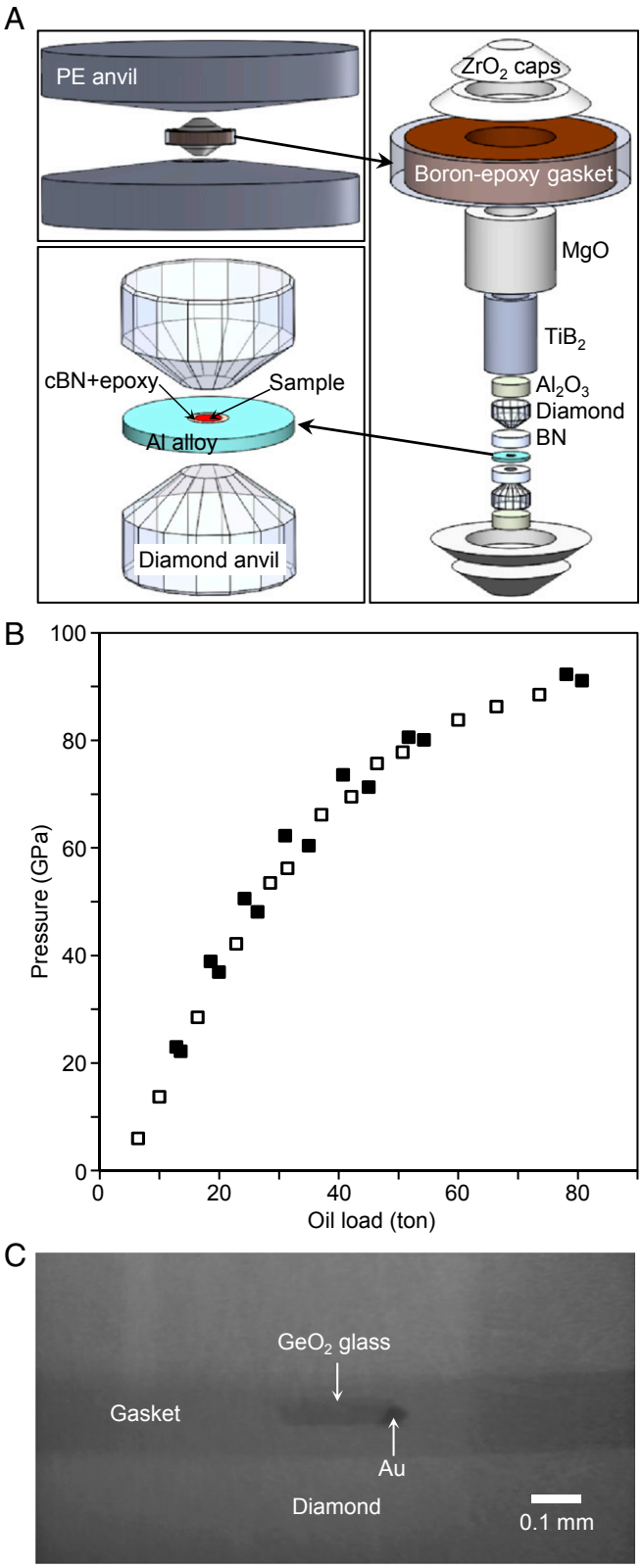

Fig. 1. Newly developed double-stage large-volume cell. (*A*) Illustration of double-stage large-volume cell design. We use cup-shaped PE-type anvil as the first-stage anvil, and the second-stage diamond anvil is introduced inside the large-volume cell assembly. (*B*) Pressure generation as a function of oil load of the PE press. Solid symbols represent pressure conditions of structure measurement of GeO_2 glass measured before and after structural measurement. Oil pressure was found to decrease slightly after each measurement, whereas sample pressure increased slightly. Error of pressure is smaller than the size of the symbol. (*C*) X-ray radiography image of the GeO_2 glass sample and Au pressure standard through gasket at 91.7 GPa.

gasket with an aluminum alloy (7075) outer gasket, both of which are low X-ray absorbing, light-element materials. The diamond anvils had a culet diameter of 0.8 mm. The large culet size allowed us to use large samples 0.3 mm in diameter and 0.15 mm in height. In our study on structure of GeO_2 glass, this new double-stage cell has reached pressures up to 91.7 GPa (Fig. 1*B*), where sample size was ∼0.24 mm in diameter and ∼0.06 mm in height, as determined by in situ X-ray radiography imaging (Fig. 1*C*).

Structure of GeO_2 glass was investigated using the newly designed double-stage PE press with multiangle energy dispersive X-ray diffraction technique at Beamline 16-BM-B, High Pressure Collaborative Access Team (HPCAT) of the Advanced Photon Source (18). Structure factors, S(Q), were obtained up to 13 $Å^{-1}$ (Fig. 2). The position of the first sharp diffraction peak (FSDP) in S(Q) shows essentially no pressure dependence between 22.6 and 37.9 GPa. Previous studies (3, 19) show that below ∼10 GPa, FSDP moves rapidly with increasing pressure toward higher Q values; above 10 GPa, the position becomes virtually pressure independent. This is consistent with our observation that the FSDP shifts rapidly from 0 to 22.6 GPa, and then remains almost constant between 22.6 and 37.9 GPa (Fig. 2). Interestingly, with further increase of pressure to 72.5 GPa, the FSDP begins shifting again toward higher Q and then becomes virtually constant once more between 72.5 and 91.7 GPa. Furthermore, a new peak at Q ∼ 7.1–7.3 $Å^{-1}$ begins to emerge at a pressure between 22.6 and 37.9 GPa, with increasing intensity at higher pressures.

Fourier transformation of S(Q) yields real-space pair distribution function (20), G(r) (Fig. 3). The first and second peak of G(r) in GeO_2 glass is generally considered to represent Ge–O and Ge–Ge distance, respectively. Significant changes in peak shape and positions in G(r), particularly in the second peak, are evident. G(r) obtained at 22.6 and 37.9 GPa show a distinct shoulder at the lower "r" side of the second peak. This shoulder has been observed in previous studies (1, 3, 5) at pressures higher than ∼15 GPa. This double-peak feature is considered to represent two Ge–Ge distances in the sixfold-coordinated GeO_2 structure. In contrast, we find that the second peak starts to become a single peak above 49.4 GPa. The second peak width markedly decreases between 37.9 and 49.4 GPa, although the second peak in G(r) at 49.4 and 61.4 GPa still shows a weak shoulder at the low-r side. The second peak becomes a single peak above 72.5 GPa.

Fig. 4 shows the pressure dependence of the first and second peak positions in G(r), with the numerical results summarized in Table 1. We fit the second peak at 22.6–61.4 GPa by two peaks, whereas those at higher pressures are fitted by a single peak. The first peak position in G(r) decreases between 22.6 and 37.9 GPa, whereas it is almost constant or increases slightly between 37.9 and 61.4 GPa. In contrast, above 72.5 GPa, the first peak position decreases markedly to ∼1.81 Å. The second peak position also shows marked change with increasing pressure. The main second peak position at ∼3.2 Å is almost constant between 22.6 and 37.9 GPa, whereas it decreases markedly with increasing pressure above 49.4 GPa.

Our results reveal that a distinct change in the structure of GeO_2 glass begins at a pressure between 37.9 and 49.4 GPa. Below 37.9 GPa, our structural data are similar to those obtained around 15–18 GPa in previous studies (1, 3, 5). Because the first and second peak positions of G(r) in GeO_2 glass are considered to represent Ge–O and Ge–Ge distances, respectively, we compare the first and second peak positions of G(r) obtained in this

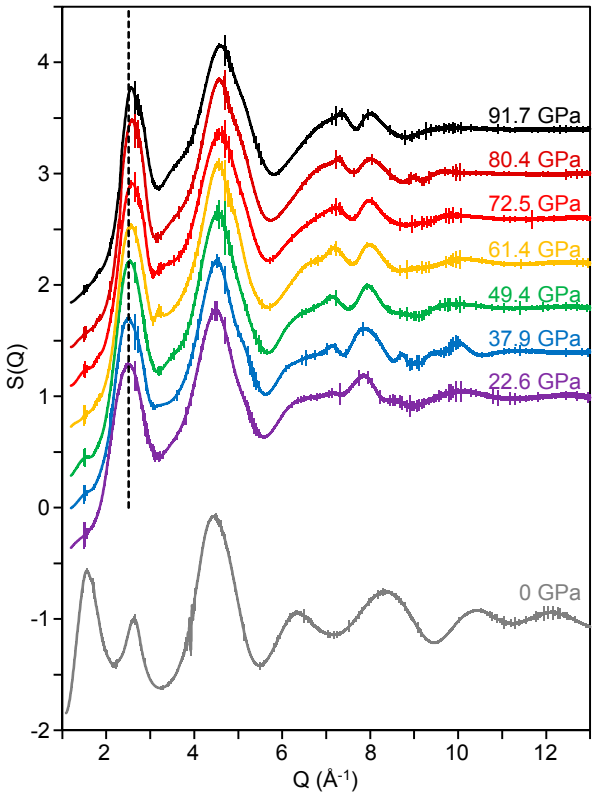

Fig. 2. Structure factor, S(Q), of GeO_2 glass up to 91.7 GPa. S(Q) was determined at the Q range up to 13 $Å^{-1}$. S(Q) at high pressure is displayed by a vertical offset of 0.4, with varying pressure, and S(Q) at ambient pressure is displayed by a vertical offset of −2. The dotted line is plotted at the first peak position at 22.6 GPa to guide the eyes. The first peak position is almost the same at 22.6 and 37.9 GPa, whereas it shifts to high Q at 49.4–72.5 GPa.

study with Ge–O and Ge–Ge bond distances of crystalline GeO_2 with sixfold-coordinated $CaCl_2$-type structure (21) (Fig. 4). Previous studies argue that two distinct peaks in G(r) between 2.5 and 3.5 Å above ∼15 GPa are an indication of formation of sixfold-coordinated structural motifs (1, 3, 5). Our comparison also shows that the double-peak positions at 22.6 and 37.9 GPa are consistent with two Ge–Ge bond distances in $CaCl_2$-type structured crystalline GeO_2 (21) (Fig. 4*B*). In addition, the first peak position is similar to the median value of the two Ge–O distances of $CaCl_2$-structured GeO_2 (Fig. 4*A*). These observations strongly suggest that structure of GeO_2 glass between 22.6 and 37.9 GPa is sixfold coordinated similar to $CaCl_2$-type structured GeO_2.

At higher pressures, the double peak in G(r) merges into a single one above 49.4 GPa (Fig. 3). Crystalline GeO_2 is known to transform to α-PbO_2-type structure at 44 GPa (22) and to pyrite-type structure at pressures between 60 and 85.8 GPa (23). At 40 GPa, α-PbO_2-type crystalline GeO_2 is composed of three Ge–O bonds (1.772, 1.814, and 1.860 Å) and three Ge–Ge distances (2.817, 3.202, and 3.2658 Å) (24). The pyrite-type GeO_2 is composed of rhombohedral polyhedra with a six-coordination structure plus two additional oxygens. At 70 GPa, the six Ge–O bonds are 1.800 Å in length, but two additional oxygen atoms are at much longer Ge–O distance of 2.622 Å (24, 25). The Ge–Ge distance is a single value (3.115 Å) (25), which is similar to the obtained second peak position in G(r) of GeO_2 glass at 72.5 GPa (Fig. 4*B*). However, we found no peak in G(r) corresponding to the longer Ge–O distance at ∼2.6 Å in the pyrite-type GeO_2 (Figs. 3 and 4). These data suggest that GeO_2 glass above 49.4 GPa has a structure which differs from the known crystalline structures under similar pressure conditions.

Ge–O coordination number can be quantitatively estimated by integrating the first peak of the radial distribution function:

$$\mathrm{CN} = 2\int_{r_0}^{r_{max}} 4\pi r^2 \rho G(r)dr,$$

where r_0 and r_{max} are the left edge position and the peak position of the first peak, respectively, and ρ is number density. To estimate the density of GeO_2 glass at high pressure, we used the third-order Birch–Murnaghan equation of state of the GeO_2 glass (ρ_0 = 4.5 g/cm^3, K_0 = 35.8 GPa, K_0' = 4), which was determined at pressures between 15 and 56 GPa (11, 26). The obtained CN results are summarized in Table 1 and Fig. 5. Previous studies report that CN of GeO_2 glass gradually increases from 4 to 6 with increasing pressure (1, 3, 5, 27), and reaches a value of 6 above ∼15 GPa (1, 5). Similarly, our data show CN of ∼6 between 22.6 and 37.9 GPa (Fig. 5). Remarkably, at higher pressures CN increases to 6.4 at 49.4 GPa, and continues to increase with pressure, reaching the highest CN of 7.4 at 91.7 GPa.

Because the density data of GeO_2 glass were measured up to 56 GPa, extrapolation of the equation of state to higher pressures may result in uncertainties in the determination of CN. We note that our extrapolation of the equation of state of GeO_2 glass yields densities of GeO_2 glass higher than those of crystalline GeO_2 with pyrite-type structure above 70 GPa. To assess the influence of density on the determination of CN, we calculated CN by using the density of pyrite-type crystalline GeO_2 (24, 25) at pressures higher than 70 GPa. This yields ∼5% lower density

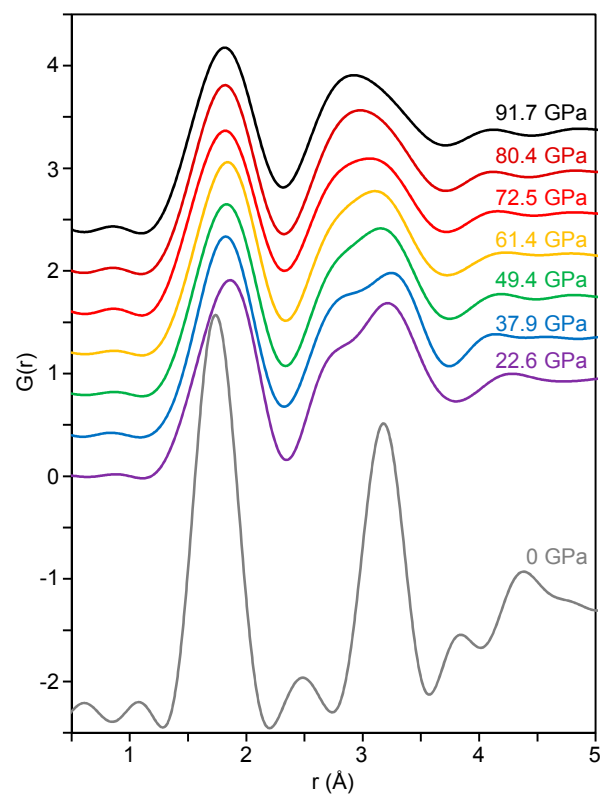

Fig. 3. Pair distribution function, G(r), of GeO_2 glass up to 91.7 GPa. G(r) at high pressures are displayed by additional vertical offset of 0.4, with varying pressure, and that at ambient pressure is displayed by an offset of −2.3. G(r) at 22.6 and 37.9 GPa show distinct two shoulders in the second peak, which is considered as an evidence of sixfold-coordinated GeO_2 glass structure (1, 3, 5), whereas it gradually becomes a single peak above 49.4 GPa.

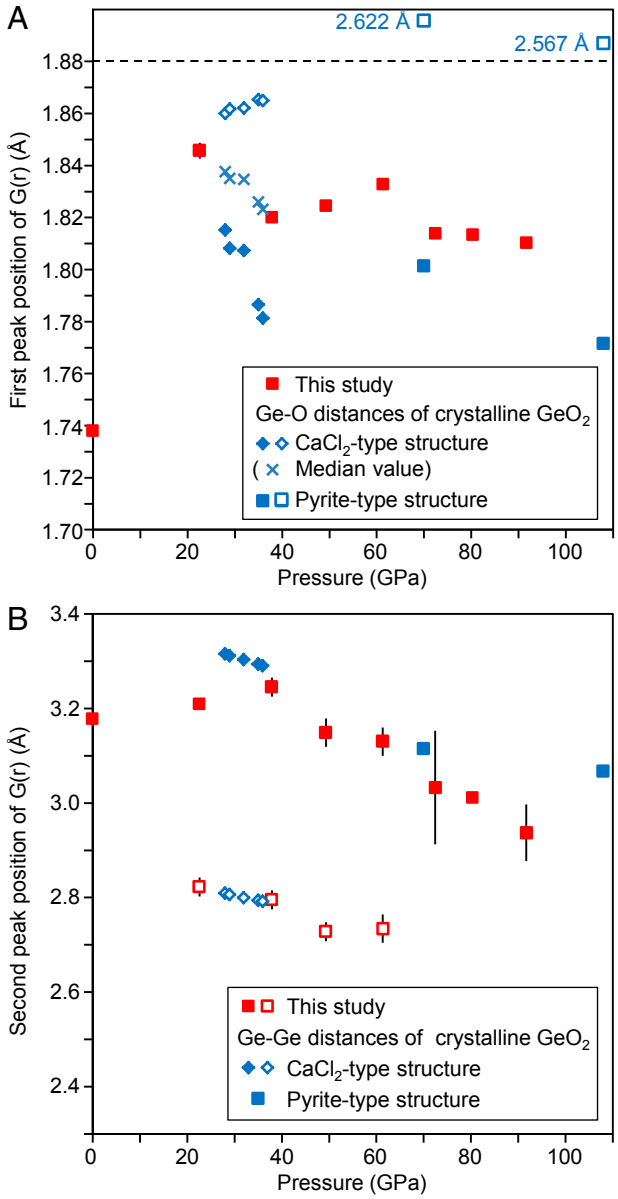

Fig. 4. The first and second peak position of G(r). (*A*) The first peak position of G(r) of GeO_2 glass obtained in this study (solid red squares), compared with Ge–O bond distance of crystalline GeO_2 with $CaCl_2$-type structure (21) (open and solid blue diamonds) and pyrite-type structure (24) (open and solid blue squares). Blue cross symbols represent the median value of the two Ge–O bond distances in $CaCl_2$-type GeO_2. Error is smaller than the size of the symbol. (*B*) The second peak position of G(r) of GeO_2 glass obtained in this study (red squares), compared with Ge–Ge bond distance of crystalline GeO_2 with $CaCl_2$-type structure (21) (open and solid blue diamonds) and pyrite-type structure (24) (solid blue square). Solid red squares represent the main second peak (r2) and open red squares represent shoulder peaks in the second peak at ~2.7–2.8 Å (r2s) (Table 1). Vertical bars represent errors of the peak positions.

at 91.7 GPa than the extrapolated GeO_2 glass density values. If we adopt the density value of pyrite-type structure crystalline GeO_2 at 72.5–91.7 GPa, CN becomes almost constant around 7. To precisely determine CN of GeO_2 glass and to discuss the change of CN with increasing pressure, precise density data particularly above 70 GPa are required. Nevertheless, our structural results provide strong evidence of GeO_2 glass possessing an ultrahigh-pressure polyamorphic structure with CN >6 above 49.4 GPa.

A recent study (7) shows that the CN of network-forming structural motifs in oxide glasses and liquids can be rationalized in terms of the OPF. Because of the lack of experimental data with CN >6, the reported data (7) are limited to 3 < CN < 6. We can now extend the relationship between CN and OPF to ultradense glasses and liquids. We calculate OPF (η_O) by using the same method as given by ref. 7 [$\eta_O = V_O \rho c_O$, $V_O = (4/3)\pi r_O^3$, where r_O is the oxygen radius, and c_O is the atomic fraction of oxygen] (i.e., assuming oxygen atoms are perfect spheres). r_O of GeO_2 glass at 22.6 and 37.9 GPa and crystalline GeO_2 with CN = 6 are calculated by assuming an octahedral geometry ($r_O = r_{GeO}/\sqrt{2}$) in the same way as ref. 7. For GeO_2 glass with CN >6, similar to the linear dependence of r_O between four- and sixfold-coordinated structures assumed in ref. 7, OPF is calculated by assuming a linear change of r_O between sixfold-coordinated structure and the ninefold-coordinated cotunnite-type structure, which is the next higher-pressure form in crystalline GeO_2 having a uniform CN >6, predicted by first-principles calculations (28). To estimate the oxygen radius for the possible CN = 9 structure motif of GeO_2 glass, we first calculate the average O–O distance (‹O–O›) of the crystalline cotunnite-type GeO_2, which consists of 21 O–O bonds at 1.929 (×2), 1.940 (×4), 1.948 (×4), 1.991 (×2), 2.055 (×2), 2.161 (×2), 2.243 (×2), and 2.540 (×3) Å, respectively (28). The oxygen radius r_O for cotunnite-type GeO_2 is then simply r_O=‹O–O›/2. Uncertainty of this r_O is assumed to be 1σ SD of ‹O–O›/2. Uncertainty in OPF is estimated based on error propagation. For estimating r_O of GeO_2 glass with CN >6, we calculated the r_O/r_{GeO} ratio (0.603) of crystalline cotunnite-type structure using its average Ge–O distance (1.735 Å) (28), and then, r_O of GeO_2 glass with CN = 9 structure motif is estimated from the measured Ge–O distances of GeO_2 glass at 49.4–91.7 GPa (Fig. 4*A*) by using r_O/r_{GeO} = 0.603. Uncertainties in the r_O/r_{GeO} ratio due to 1σ SD in r_O of the cotunnite-type GeO_2 are adopted as errors in r_O and the resultant OPF of GeO_2 glass with CN >6.

Fig. 6 shows CN as a function of OPF extended to CN >6, combined with the data of GeO_2 glass for 4 < CN < 6 (7). Ref. 7 showed that fourfold-coordinated GeO_2 glass is stable in a wide range of OPF up to ~0.60 (Fig. 6). CN begins increasing when OPF approaches ~0.60. The positive correlation between CN and OPF continues until OPF reaches ~0.64. Then CN sharply increases to 6, with OPF remaining essentially constant at ~0.64. At pressures of 22.6 and 37.9 GPa, OPF of GeO_2 glass increases, with CN remaining almost constant at 6 (Fig. 6). This is a stable plateau for sixfold-coordinated structure, similar to the plateau for CN = 4. The sixfold-coordinated GeO_2 glass is structurally stable in a wide range of OPF between ~0.64 and ~0.71, similar to the behavior of sixfold-coordinated SiO_2 glass (7). Then, the CN of GeO_2 glass increases to 6.4 at OPF = 0.72. At higher pressures, CN increases further to CN = 7.4 at 94 GPa, while OPF remains essentially constant at ~0.72 (Fig. 6).

Table 1. Experimental pressure conditions and the results of the first (r1) and second peak positions of G(r), and CN

Pressure (GPa)	r1, Å	r2s, Å	r2, Å	CN
0.0	1.738 ± 0.001		3.177 ± 0.01	4.0 ± 0.2
22.6 ± 0.4	1.846 ± 0.003	2.823 ± 0.02	3.209 ± 0.01	5.8 ± 0.2
37.9 ± 1.0	1.820 ± 0.001	2.795 ± 0.02	3.245 ± 0.02	5.9 ± 0.2
49.4 ± 1.3	1.824 ± 0.001	2.728 ± 0.02	3.149 ± 0.03	6.4 ± 0.2
61.4 ± 0.9	1.833 ± 0.001	2.734 ± 0.03	3.130 ± 0.03	7.0 ± 0.2
72.5 ± 1.1	1.814 ± 0.001		3.033 ± 0.12	7.0 ± 0.2
80.4 ± 0.3	1.813 ± 0.001		3.011 ± 0.01	7.1 ± 0.2
91.7 ± 0.6	1.810 ± 0.001		2.937 ± 0.06	7.4 ± 0.2

The second peaks at 22.6–61.4 GPa are fitted by two peaks for shoulder peak at ~2.7–2.8 Å (r2s) and main peak (r2).

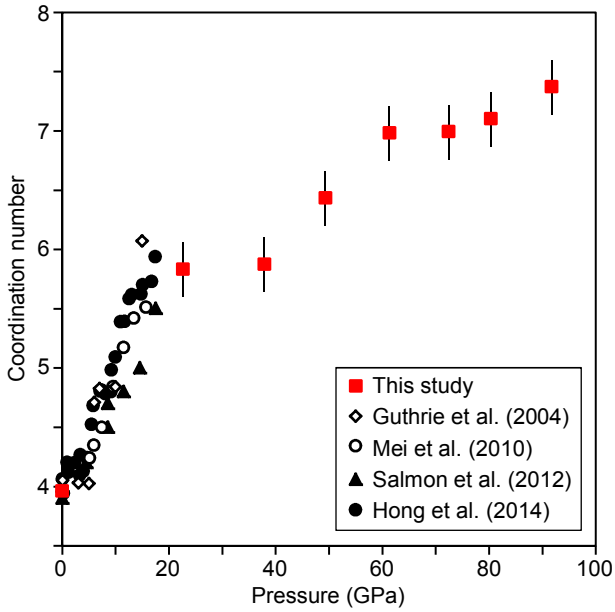

Fig. 5. Coordination number of Ge in GeO_2 glass as a function of pressure. Red squares represent results of this study, and black symbols are results of previous studies [open diamonds (1), open circles (3), solid triangles (27), solid circles (5)]. Coordination number at 22.6 and 37.9 GPa is almost constant at around 6, whereas it increases markedly to 6.4 at 49.4 GPa. Coordination number continues to increase with pressure, and the highest coordination number of 7.4 is observed at 91.7 GPa. Vertical bars represent errors of coordination number. Error of pressure is represented by the size of the symbols.

Ref. 7 has shown that the CN and OPF relationship is "universal" in many network-forming glasses and liquids such as SiO_2, GeO_2, silicate, aluminate, and germanate systems at high pressures in the CN range between 3 and 6. For example, for SiO_2 glass, the fourfold-coordinated structure is stable at OPF up to ~0.55–0.60 (7). At OPF >~0.60, CN of SiO_2 glass increases to 6, and the sixfold-coordinated structure is stable at the OPF up to ~0.72 (7). The CN–OPF relation for SiO_2 coincides with that of GeO_2 as illustrated by the gray band in Fig. 6. Although experimentally determined highest CN in SiO_2 glass is 6 at 101.5 GPa (4), similar to crystalline GeO_2, a cotunnite-type structure is also known as the next high-pressure form for crystalline SiO_2 having a uniform CN of 9 (29, 30). OPF of the cotunnite-type SiO_2 (30), calculated using the same method as GeO_2, is 0.71, similar to that of cotunnite-type GeO_2. Thus, similar to GeO_2 glass, SiO_2 glass may also change structure toward CN = 9 at higher pressure conditions. In addition to SiO_2 glass, the relation between CN and OPF in basalt melt also follows the same curve with CN between 4 and 6 (7), further confirming that the CN–OPF relationship describes a master curve for predicting structural changes in glasses and liquids at high pressure.

Our data on GeO_2 show that structural changes in glasses and liquids are closely associated with hard-sphere packing even to higher coordination numbers. Fourfold-coordinated structures are stable with OPF up to 0.55–0.60, corresponding to random loose packing of hard spheres (8, 9). Further compression increases CN sharply to 6 at OPF of ~0.64, which is the most-disordered random closed-packing limit of hard spheres (8, 9), known as the maximally random jammed (MRJ) state (29) (Fig. 6). Our data show that there is a stable plateau for the sixfold-coordinated structure at OPF between ~0.64 and ~0.72. OPF of ~0.72 is close to the maximal dense-packing state [the Kepler conjecture(KC) = ~0.74, ref. 31], where a certain degree of local ordering, relative to the MRJ state, must be involved (32). Structure evolves to higher CN with OPF remaining essentially constant just below the KC state packing limit (~0.74).

This extended CN versus OPF relation provides new insights into structural changes in other glasses and liquids under extreme compression. For SiO_2 glass, experimentally determined highest CN is 6 at 101.5 GPa (4). The number density (0.154/$Å^{-3}$) and Si–O distance (1.67 Å) at 101.5 GPa (4) yield OPF = 0.71, which is still lower than that of the KC packing state. OPF of SiO_2 glass with CN = 6, calculated based on the results of ref. 4, increases from ~0.68 at 35.2 GPa to ~0.71 at 101.5 GPa (Fig. S1). If we linearly extrapolate the OPF–pressure trend, OPF of SiO_2 glass reaches 0.74 around 108 GPa, where structural change to CN higher than 6 is expected. We expect that further compression of silica (and likely other silicate glasses and liquids) should follow the dashed gray band shown in Fig. 6 toward higher CN.

Methods

The new double-stage large-volume cell is developed in a 200-ton PE press. We used a cup-shaped anvil with 12-mm cup diameter with 3-mm flat bottom as the first-stage anvil and (100)-oriented single-crystal diamond with 0.8-mm culet as the second-stage anvil. The gasket is composed of a cubic boron nitride + epoxy (10:1 in weight ratio) inner gasket with an aluminum alloy (7075) outer gasket. Initial sample size is 0.3 mm in diameter and 0.15 mm thick. A GeO_2 glass sample was packed in the gasket hole without pressure medium to avoid diffraction peaks from pressure medium in the X-ray diffraction measurement. A piece of Au (cut from 0.05-mm-diameter wire) is placed as a pressure standard at the sample edge to avoid contamination of X-ray diffraction signal from Au into X-ray spectrum of GeO_2 glass sample. Pressures were determined by the equation of state of Au (33). We measured pressure before and after structure measurement of glass because of long measurement time (~4.5 h). Pressure difference before and after structure measurement was up to 2.5 GPa. Table 1 shows the average pressures obtained before and after measurements with the pressure differences as errors. Pressure gradient between the center and edge of sample was up to 4 GPa at pressures up to 93.4 GPa obtained in a separate experiment using MgO and Au as samples.

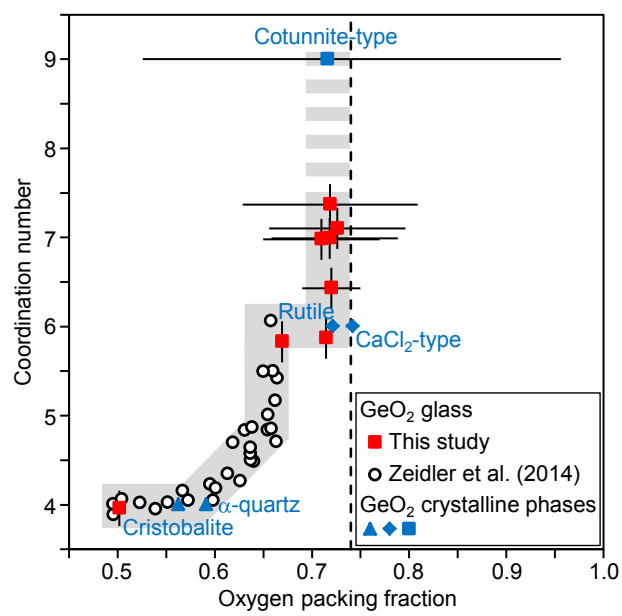

Fig. 6. Relationship between the OPF and the coordination number of Ge. GeO_2 glass data from this study (solid red squares) and from ref. 7 (open black circles) are compared with those of GeO_2 crystals with coordination numbers of 4 (cristobalite and alpha quartz, ref. 7) (blue triangles), 6 (rutile and $CaCl_2$ structures, ref. 21) (blue diamonds), and 9 (cotunnite-type structure, ref. 28) (blue square). OPF was calculated by using the method of ref. 7. Vertical broken line represents the maximal dense-packing state (KC = ~0.74, ref. 31).

Structure of GeO_2 glass was investigated using the multiangle energy-dispersive X-ray diffraction technique (18). We used unfocused white X-rays. The size of incident white X-ray is 0.1 mm in both horizontal and vertical directions. We collected series of energy-dispersive X-ray diffraction patterns at 2θ angles of 4°, 5°, 7°, 9°, 12°, 16°, 21°, and 29° using a Ge solid-state detector (Canberra). Total exposure time to obtain the X-ray diffraction patterns for eight 2θ angles was about 4.5 h. Structure factor was derived from the observed energy-dispersive X-ray diffraction patterns using the program aEDXD (18). The Kaplow-type correction using an optimization procedure (34) was applied in determining final structure factor and pair distribution function. The iteration in the optimization process is typically 3.

ACKNOWLEDGMENTS. We acknowledge two anonymous reviewers for valuable comments. This study was performed at HPCAT (Sector 16), Advanced Photon Source, Argonne National Laboratory. This research is supported by Department of Energy (DOE)-National Nuclear Security Administration under Award DE-NA0001974 and DOE-Office of Basic Energy Sciences under Award DE-FG02-99ER45775. Advanced Photon Source is a US DOE Office of Science User Facility operated for the DOE Office of Science by Argonne National Laboratory under Contract DE-AC02-06CH11357. The PE cell program is partly supported by GeoSoilEnviroCARS, which is supported by the National Science Foundation–Earth Sciences (EAR-1128799) and Department of Energy-GeoSciences (DE-FG02-94ER14466). Y.W. acknowledges support from National Science Foundation EAR-1214376.

1. Guthrie M, et al. (2004) Formation and structure of a dense octahedral glass. *Phys Rev Lett* 93(11):115502.
2. Benmore CJ, et al. (2010) Structural and topological changes in silica glass at pressure. *Phys Rev B* 81(5):054105.
3. Mei Q, et al. (2010) High-pressure x-ray diffraction measurements on vitreous GeO_2 under hydrostatic conditions. *Phys Rev B* 81(17):174113.
4. Sato T, Funamori N (2010) High-pressure structural transformation of SiO_2 glass up to 100 GPa. *Phys Rev B* 82(18):184102.
5. Hong X, Ehm L, Duffy TS (2014) Polyhedral units and network connectivity in GeO_2 glass at high pressure: An X-ray total scattering investigation. *Appl Phys Lett* 105(8):081904.
6. Kohara S, Suzuya K (2005) Intermediate-range order in vitreous SiO2 and GeO2. *J Phys Condens Matter* 17(5):S77.
7. Zeidler A, Salmon PS, Skinner LB (2014) Packing and the structural transformations in liquid and amorphous oxides from ambient to extreme conditions. *Proc Natl Acad Sci USA* 111(28):10045–10048.
8. Scott GD, Kilgour DM (1969) The density of random close packing of spheres. *J Phys D Appl Phys* 2(6):863.
9. Song C, Wang P, Makse HA (2008) A phase diagram for jammed matter. *Nature* 453(7195):629–632.
10. Baldini M, et al. (2010) High-pressure EXAFS study of vitreous GeO_2 up to 44 GPa. *Phys Rev B* 81(2):024201.
11. Hong X, Newville M, Duffy TS, Sutton SR, Rivers ML (2014) X-ray absorption spectroscopy of GeO_2 glass to 64 GPa. *J Phys Condens Matter* 26(3):035104.
12. Karki BB, Bhattarai D, Stixrude L (2007) First-principles simulations of liquid silica: Structural and dynamical behavior at high pressure. *Phys Rev B* 76(10):104205.
13. Brazhkin VV, Lyapin AG, Trachenko K (2011) Atomistic modeling of multiple amorphous-amorphous transitions in SiO_2 and GeO_2 glasses at megabar pressures. *Phys Rev B* 83(13):132103.
14. Murakami M, Bass JD (2010) Spectroscopic evidence for ultrahigh-pressure polymorphism in SiO_2 glass. *Phys Rev Lett* 104(2):025504.
15. Boehler R, et al. (2013) Large-volume diamond cells for neutron diffraction above 90 GPa. *High Press Res* 33(3):546–554.
16. Endo S, Ito K (1980) Electrical resistance of αFe2O3 under ultrahigh static pressure. *Solid State Commun* 36(2):189–190.
17. Kunimoto T, Irifune T, Sumiya H (2008) Pressure generation in a 6-8-2 type multi-anvil system: A performance test for third-stage anvils with various diamonds. *High Press Res* 28(3):237–244.
18. Kono Y, Park C, Kenney-Benson C, Shen G, Wang Y (2014) Toward comprehensive studies of liquids at high pressures and high temperatures: Combined structure, elastic wave velocity, and viscosity measurements in the Paris–Edinburgh cell. *Phys Earth Planet Inter* 228(0):269–280.
19. Hong X, et al. (2007) Intermediate states of GeO_2 glass under pressures up to 35 GPa. *Phys Rev B* 75(10):104201.
20. Kaplow R, Strong SL, Averbach BL (1965) Radial density functions for liquid mercury and lead. *Phys Rev* 138(5A):A1336–A1345.
21. Haines J, Leger JM, Chateau C, Pereira AS (2000) Structural evolution of rutile-type and CaCl2-type germanium dioxide at high pressure. *Phys Chem Miner* 27(8):575–582.
22. Prakapenka VB, et al. (2003) α-PbO_2-type high-pressure polymorph of GeO_2. *Phys Rev B* 67(13):132101.
23. Ono S, Tsuchiya T, Hirose K, Ohishi Y (2003) High-pressure form of pyrite-type germanium dioxide. *Phys Rev B* 68(1):014103.
24. Łodziana Z, Parlinski K, Hafner J (2001) Ab initio studies of high-pressure transformations in GeO_2. *Phys Rev B* 63(13):134106.
25. Shiraki K, Tsuchiya T, Ono S (2003) Structural refinements of high-pressure phases in germanium dioxide. *Acta Crystallogr B* 59(Pt 6):701–708.
26. Hong X, Shen G, Prakapenka VB, Rivers ML, Sutton SR (2007) Density measurements of noncrystalline materials at high pressure with diamond anvil cell. *Rev Sci Instrum* 78(10):103905.
27. Salmon PS, et al. (2012) Density-driven structural transformations in network forming glasses: A high-pressure neutron diffraction study of GeO_2 glass up to 17.5 GPa. *J Phys Condens Matter* 24(41):415102.
28. Dekura H, Tsuchiya T, Tsuchiya J (2011) First-principles prediction of post-pyrite phase transitions in germanium dioxide. *Phys Rev B* 83(13):134114.
29. Oganov AR, Gillan MJ, Price GD (2005) Structural stability of silica at high pressures and temperatures. *Phys Rev B* 71(6):064104.
30. Wu S, et al. (2011) Identification of post-pyrite phase transitions in SiO_2 by a genetic algorithm. *Phys Rev B* 83(18):184102.
31. Hales TC (2005) A proof of the Kepler conjecture. *Ann Math* 162:1065–1185.
32. Torquato S, Stillinger FH (2010) Jammed hard-particle packings: From Kepler to Bernal and beyond. *Rev Mod Phys* 82(3):2633.
33. Tsuchiya T (2003) First-principles prediction of the P-V-T equation of state of gold and the 660-km discontinuity in Earth's mantle. *J Geophys Res: Solid Earth* 108(B10):2462.
34. Shen G, Prakapenka VB, Rivers ML, Sutton SR (2003) Structural investigation of amorphous materials at high pressures using the diamond anvil cell. *Rev Sci Instrum* 74(6):3021–3026.

Supporting Information

Kono et al. 10.1073/pnas.1524304113

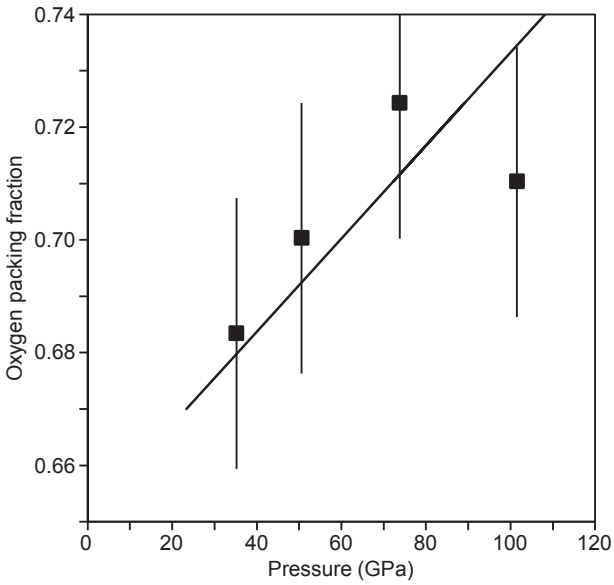

Fig. S1. OPF of SiO_2 glass with increasing pressure, calculated based on the results of Si–O distance and number density (4). Error of the OPF is calculated based on uncertainty in the Si–O distance. Linear extrapolation of the OPF–pressure trend shows that OPF of SiO_2 glass reaches 0.74 around 108 GPa.